Development and functional verification of an ultra-deep drilling core geological environment true triaxial apparatus

Xiwei Zhang
Key Laboratory of Ministry of Education on Safe Mining of Deep Metal Mines, Northeastern University, Shenyang, China

Lei Shi
Key Laboratory of Ministry of Education on Safe Mining of Deep Metal Mines, Northeastern University, Shenyang, China

ABSTRACT: Given that the drilled core diameter decreases with increasing depth and there is no true triaxial apparatus for testing the complete stress–strain behavior and long-term deformation behavior of small-sized cores, a geological environment true triaxial apparatus was developed. The apparatus was mainly designed to obtain the complete stress–strain curves of hard rock specimens measuring 25 mm×25 mm×50 mm, while also considering the measurement of long-term deformation. This device focuses on solving technical problems such as inaccurate measurement of specimen deformation, low stiffness of the apparatus, mutual interference between pressure chamber oil pressure and actuator pressure. The deformation behavior of Xiling ultra-deep drilling cores was measured using this apparatus.

Keywords: ultra-deep drilling core; true triaxial test; complete stress–strain; time-dependent failure.

1 INTRODUCTION

Ultra-deep drilling investigation is an important method to evaluate the stability of deep geological structures. The environment of ultra-deep core drilling is characterized by high *in-situ* stress, many large fault structures, and abundant local rock mass fissure water. In addition, the *in-situ* stress under the action of structural stress presents a true triaxial stress state ($\sigma_1 > \sigma_2 > \sigma_3$). Therefore, studying the mechanical behavior of ultra-deep drill cores under true triaxial stress can help the analysis of the mechanism of deep and ultra-deep geohazards.

Mogi (1971) developed the first rock true triaxial apparatus in 1971, which proved that σ_2 affects the strength and deformation of rock. In 1989, Xu et al. (1990) designed China's first rock true triaxial apparatus. The above two true triaxial apparatus can be mainly used to obtain the pre-peak failure behavior of rocks. To obtain post-peak curves of hard rock, Haimson & Chang (2000) developed a true triaxial apparatus with servo control, but only partial post-peak curves were acquired due to the limitations of the testing technique. Since 2000, some true triaxial apparatus with high stress loading capacity have been successfully developed, and the monitoring of the complete stress–strain curve of hard rock has also been achieved (Zhang et al. 2017). In addition, for the long-term failure behavior, fluid coupling failure behavior, and temperature coupling failure behavior of hard rock,

some true triaxial apparatus with corresponding functions have also been successfully developed (Nasseri et al. 2014 and Feng et al. 2018).

At present, the true triaxial compression (TTC) tests for determining complete stress-strain curves and long-time failure behavior of rocks were mainly used for specimens measuring 50 mm × 50 mm ×100 mm. However, the diameter of the obtained ultra-deep drilling geological core is too small to be processed to this size, resulting in less research being conducted into its mechanical behavior under true triaxial stress. Therefore, a true triaxial apparatus for studying ultra-deep drilled cores has been developed in the present study.

2 OVERALL DESIGN OF THE TRUE TRIAXIAL APPARATUS

The design background of this apparatus mainly considers the difficulty of obtaining ultra-deep drill cores, the small core diameter and the high scientific research value and sets the specimen size to 25 mm×25 mm×50 mm to meet ability to process most ultra-deep cores. Figure 1 shows the apparatus which is a testing machine with two-rigid and one-flexible load types. The apparatus is mainly used for investigating the complete stress–strain behavior and time-dependent deformation behavior of hard rock under three-dimensional stress state; σ_1 and σ_2 are applied rigidly by the actuator driven by the high-precision servo-driven pump, and σ_3 is applied flexibly by the high-precision servo-driven pump to pressurize the hydraulic oil in the pressure chamber. The maximum loading capacities of σ_1, σ_2, and σ_3 are 1000 MPa, 500 MPa, and 70 MPa respectively, meeting the requirements for simulation of a deep rock stress-environment. Three pressure sensors are used to monitor the pressure of the high-pressure tubing in three directions and calculate σ_1 and σ_2 of the specimen from the effective area acting on the piston. The deformation of the specimen in three directions is measured by linear variable differential transformer (LVDT) sensors. The EDC controllers collect the sensor signal and send the pressure signal or deformation signal as the feedback signal to the servo-motor drive pump to form a closed-loop servo-motor control working mode.

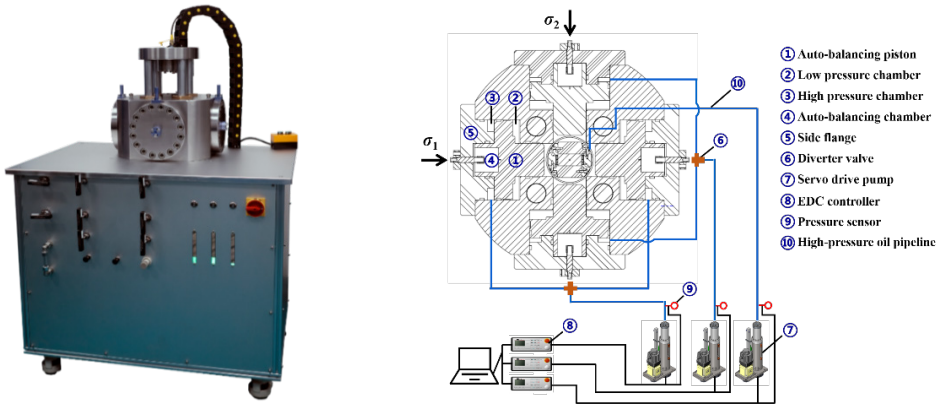

(a) (b)

Figure 1. The (a) physical diagram and (b) schematic diagram of ultra-deep drilling core geological environment true triaxial apparatus.

3 KEY TECHNOLOGY UNDERPINNING THE TRUE TRIAXIAL APPARATUS

3.1 Accurate measurement of rock deformation

To avoid the interference between adjacent loading briquettes, the rigid loading direction of the conventional true triaxial apparatus usually uses a smaller loading briquette than the specimen, which leads to a loading gap in the specimen. During the loading process, the stress concentration occurs at the loading gap of the specimen, which affects the deformation, strength, and failure mode of the

specimen. To solve this problem, this apparatus uses overlapping platens in the σ_1 and σ_2-directions, which can be interleaved during loading to cover the specimen (Fig. 2). The σ_3-direction and the adjacent platens are filled with sealant to prevent the high-pressure oil from penetrating the specimen during the test.

In the TTC tests, the deformation of the specimen in three directions should be measured separately. In addition, a sliding type orthogonal deformation LVDT sensor precision measurement structure was designed for use in the σ_1 and σ_2-directions due to the existence of reverse tiny parallel sliding of the overlapping platens in the same direction during the test (Fig. 2a). The structure consists of a disc-type spring-loaded telescoping rod and an LVDT sensor body. It is measured by a stylus contact on the opposite side. The stylus drives the telescopic rod of the LVDT sensor to move when the rock is deformed, thus realizing measurement of the deformation of the specimen in the σ_1 and σ_2-directions. The σ_3-direction is the glued surface of the specimen; for this reason, a fixed single-span beam LVDT sensor precision measurement structure is designed in the σ_3-direction (Fig. 2b). The structure comprises a metal rod, a positioning block, and the LVDT sensor body. The positioning block on one side of the specimen is fixed in the position to the metal rod by screws, and the positioning block on the other side touches the embedded LVDT sensor. When the σ_3-direction of the specimen is deformed, the position of the positioning block changes and the telescopic rod of the sensor moves, thus realizing deformation measurement in the σ_3-direction of the specimen.

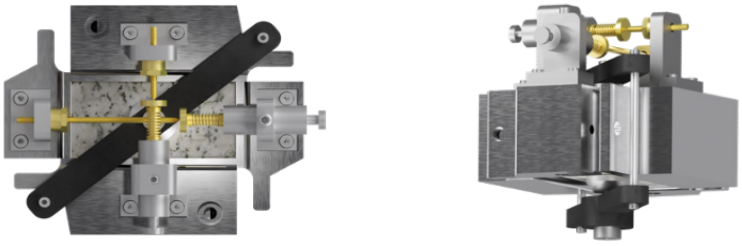

(a) (b)

Figure 2. (a) Front view and (b) side view of overlapping platens-specimen-deformation sensors combination.

In the TTC tests, the friction between the loading briquettes and the specimen affects the accuracy of the test results, that is, the end-friction effect. To achieve a uniform stress distribution in the specimen, a mixture of stearic acid and Vaseline in a 1:1 ratio (Feng et al. 2017) was applied along the metal-rock interface to reduce friction.

3.2 High-stiffness loading frame

Currently, the TTC tests mainly use the loading frame to provide the reaction forces corresponding to σ_1 and σ_2 as well as a separate pressure chamber to generate σ_3. This structure reduces the integration of the apparatus and thus loses the stiffness of the apparatus. For this purpose, a novel confining pressure cell-loading frame-hydraulic actuator counter-force frame structure was designed (Fig. 3). The structure has four stepped holes machined around the perimeter, and four pistons are installed in the stepped holes, which are sealed with the stepped holes by O-rings and side flanges to form four integrated hydraulic actuators. Four hydraulic actuators serve to seal the square structure and apply rigid loading. This structure has a stiffness of 10 GN/m, much greater than the 5 GN/m proposed by the ISRM (Fairhurst et al. 1999).

3.3 Long-term stable loading technology

In traditional TTC tests, the electro-hydraulic servo valve is used to control the oil volume of the actuator to improve the response frequency of the actuator, and the hydraulic oil source is used to provide the required flow and pressure for the electro-hydraulic servo valve. However, the hydraulic oil source generates significant heat, resulting in the safe working time of the test system being less

than 24 hours. For this reason, the apparatus contains a high-precision servo-motor drive pump as the power source. The high-accuracy servo-motor drive pump has the ability of boosting and long-term stable low-power loading, and the rating of its internal servo-motor is as low as 1 kW. Under the condition of continuous power supply, the apparatus can operate stably for six months.

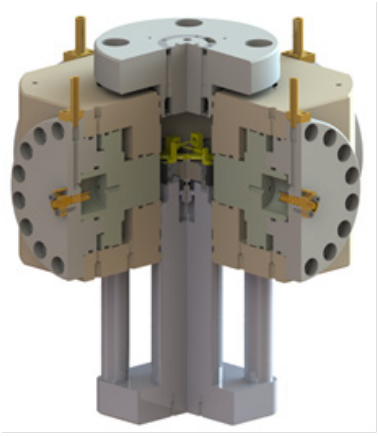

Figure 3. The confining pressure cell-loading frame-hydraulic actuator counter-force frame structure.

The apparatus uses the pressure chamber as the outer cylinder to design four built-in hydraulic actuators. The four pistons are of the same specification and are of a double-acting type. The pistons are installed in the step holes to form three chambers, namely, a low-pressure chamber, a high-pressure chamber, and a self-balancing chamber (Fig. 1(b)). The low-pressure chamber is connected to the air compressor to assist in unloading the piston to the original position after the test. The high-pressure chamber is connected to a high-precision servo displacement pump, which drives piston loading. The high-pressure oil pipe of the high-pressure chamber is fitted with a pressure sensor with an accuracy of ± 1%. Two actuators in the same principal stress direction are loaded by a high-precision servo-motor displacement pump and a synchronized, balanced pressure supply is realized through the diverter valve, which prevents eccentricity of loading on the specimen after long-term loading with the coaxial actuators. In addition, the center of the piston is equipped with a self-balancing through hole connecting the pressure chamber and the self-balancing chamber with a diameter of 10 mm, so as to ensure that the hydraulic oil in the pressure chamber is injected into the self-balancing chamber, so as to ensure that the force on the two indenter faces in the horizontal direction of the piston are equal, and ensure that the output force of the rigid hydraulic actuator is the deviator stress (σ_1-σ_3 and σ_2-σ_3) The mutual interference between the high oil pressure in the pressure chamber and the output force of the actuator is thus overcome.

4 DEFORMATION BEHAVIOR OF HARD ROCK

4.1 Complete stress–strain behavior of hard rock

TTC tests were performed on granite, basalt, marble, and sandstone to obtain complete stress–strain curves for these rocks. The loading path is: the specimen was first loaded hydrostatically to σ_3. Then, σ_1 and σ_2 were simultaneously increased to the desired σ_2 while σ_3 remained unchanged. Finally, σ_1 was increased while both σ_2 and σ_3 remained unchanged. The stresses were applied under load control at a rate of 0.5 MPa/s in all the three stages until the stress–strain curve showed yield. After that, the loading was changed to deformation control using the σ_3 direction as the servo control feedback signal at a rate of 0·003 mm/min.

Figure 4 shows the complete stress–strain curves of four hard rocks under TTC. The pre-peak behavior of granite and basalt shows good elastic deformation characteristics, and the post-peak behavior presents Class II curve characteristics (Shi et al. 2023), and there are multi–stage stress drops, consistent with the brittle fracture characteristics of Class II rock (Figs. 4(a) and (b)). The pre-

peak curves of marble and sandstone exhibit plastic yield characteristics, and the post-peak curves are Class I curves, which can be loaded to the residual strength (Figs. 4(c) and (d)). These results show that the apparatus can be used to obtain the complete stress–strain curve of hard rock specimens.

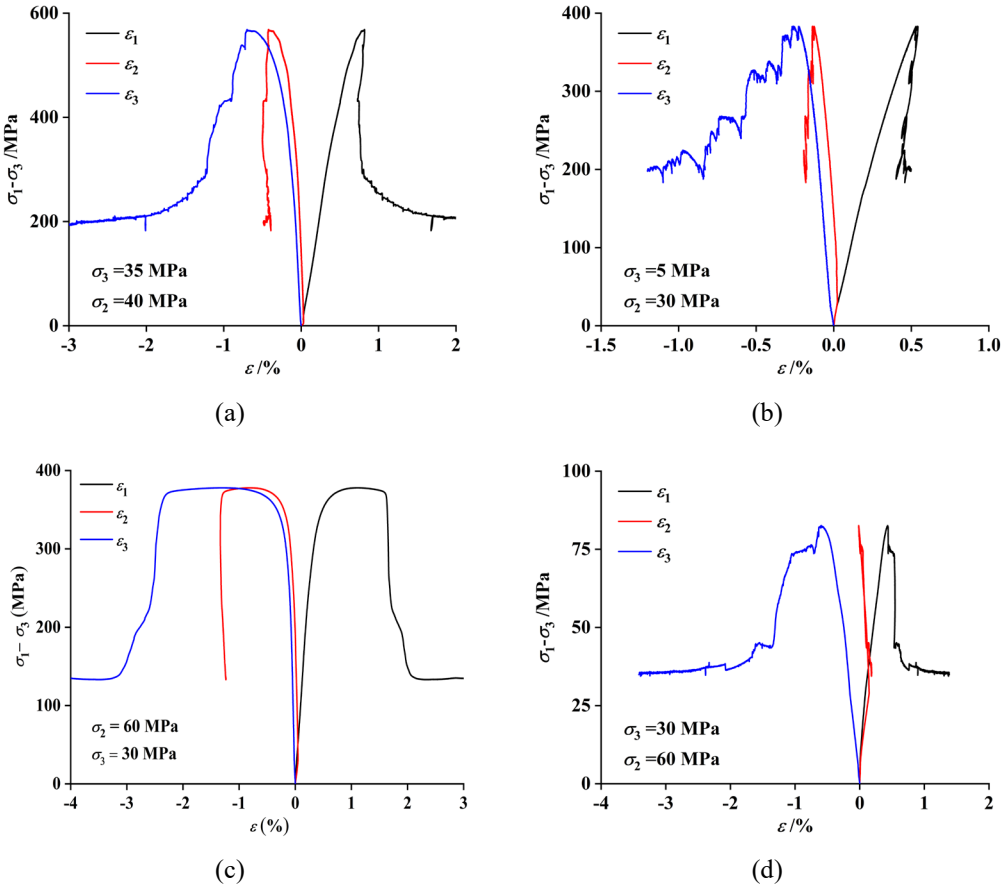

Figure 4. Complete stress–strain curves of typical hard rock specimens under TTC: (a) granite, (b) basalt, (c) marble and (d) sandstone.

4.2 Deformation behavior of hard rock under multi-stage true triaxial creep tests

In the multi-stage true triaxial creep tests, the three principal stresses were loaded under stress control (the loading rate was 0.5 MPa/s). The loading of σ_3 and σ_2 is as described in the TTC, and σ_1 is applied in a multi-stage manner: each stage is maintained for 48 hours.

Figure 5 shows the deviatoric stress–strain–time curves of a granite specimen under multi-stage true triaxial creep test conditions. The deviatoric stress–time curve shows that the whole test has been conducted in four stages, lasting 158.7 hours, and the deviatoric stress at each stage is stable with excellent load-holding, which shows that the long-term load-holding capacity of the apparatus is reliable. The strain–time curves show that the strains in the three directions all exhibit three stages of decay creep, steady creep, and accelerated creep. In addition, at the end of the test, ε_1, ε_2, and ε_3 are 0.92%, -0.41%, and -1.4%, respectively, indicating that the true triaxial stress-induced deformation in three directions of the Xiling granite specimen demonstrates anisotropy.

5 CONCLUSION

In present study, an ultra-deep drilling core geological environment true triaxial apparatus was developed, which can obtain the complete stress–strain behavior and long-term deformation behavior of a specimen measuring 25 mm × 25 mm × 50 mm. This apparatus adopts the two-rigid and one-

flexible load type to realize the loading of σ_1, σ_2, and σ_3, and the maximum loading capacity of the three principal stresses is 1000 MPa, 500 MPa, and 70 MPa, respectively. The reliable function of the apparatus is proved by testing the complete stress–strain behavior and long-term deformation behavior of hard rock specimens.

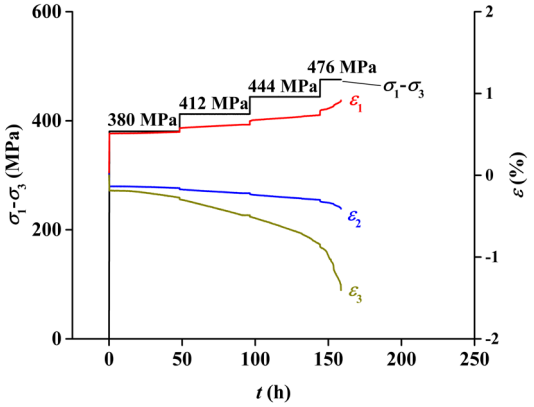

Figure 5. Deviatoric stress–strain–time curves of a granite specimen under multi-stage true triaxial creep.

REFERENCES

Fairhurst, C.E., & Hudson, J.A. 1999. Draft ISRM suggested method for the complete stress–strain curve for intact rock in uniaxial compression. *International Journal of Rock Mechanics and Mining Sciences* 36 (3), pp. 279–289.

Feng, X.T., Zhang, X., Yang, C., Kong, R., Liu, X., & Peng, S. 2017. Evaluation and reduction of the end friction effect in true triaxial tests on hard rocks. *International Journal of Rock Mechanics and Mining Sciences* 97, pp. 144–148.

Feng, X.T., Zhao, J., Zhang, X. & Kong, R. 2018. A novel true triaxial apparatus for studying the time-dependent behaviour of hard rocks under high stress. *Rock Mechanics and Rock Engineering* 51 (9), pp. 2653–2667.

Haimson, B. & Chang, C. 2000. A new true triaxial cell for testing mechanical properties of rock and its use to determine rock strength and deformability of Westerly granite. *International Journal of Rock Mechanics and Mining Sciences* 37 (1), pp. 285–296.

Mogi, K. 1971. Effect of the triaxial stress system on the failure of dolomite and limestone. *Tectonophysics* 11 (2), pp. 111–127.

Nasseri, M.H.B., Goodfellow, S.D., Lombos, L. & Young R.P. 2014. 3-D transport and acoustic properties of Fontainebleau sandstone during true-triaxial deformation experiments. *International Journal of Rock Mechanics and Mining Sciences* 69, pp. 1–18.

Shi, L., Li, C.C., Zhang, X. & Feng, X.T. 2023. Experimental verification of the intrinsic strainburst proneness of various rock types. *Bulletin of Engineering Geology and the Environment* 82 (4). pp. 119.

Xu, D., Xing, Z., Li, X, Zhang, G. & Wei, M. 1990. Development of RT3 type rock high pressure true triaxial machine. *Rock and Soil Mechanics* 11 (2), pp. 1–14.

Zhang, X., Feng, X., Kong, R., Wang, G. & Peng, S. 2017. Key technology in development of true triaxial apparatus to determine stress-strain curves for hard rocks. *Chinese Journal of Rock Mechanics and Engineering* 36(11), pp. 2629–2640.